Analysis Of Slag From The Coal-Fired Flow Facility

Author(s): C. Jiang, M. Li, C. F. Martin, and J. T. Lineberry

Session Name: Downstream Components

SEAM: 28 (1990)

SEAM EDX URL: https://edx.netl.doe.gov/dataset/seam-28

EDX Paper ID: 1423

ANALYSIS OF SLAG FROM THE COAL FIRED FLOW FACILITY*

Jiang Chi Zhi, Li Mao, C. F. Martin and J. T. Lineberry

The University of Tennessee Space Institute
Tullahoma, TN

ABSTRACT

Results of analysis of slag samples taken from the CFFF are presented. During 1989, a multitude of post test samples of slag deposits was collected from the walls of various components of the upstream CFFF test train after completion of long duration tests. These samples were extracted from many, distributed locations along the test train. The physical characteristics of these samples were qualitatively evaluated. Discussions are included which summarize these findings. A comparison of the slag deposits to experimental heat transfer data and plasma dynamics at varying location along the length of the CFFF test train is made. Qualitative analyses of the samples were also made in the CFFF chemical laboratory using the Scanning Electron Microscope. These laboratory studies were directed at determination of the slag chemical composition, structure and texture. Particular emphasis was placed upon quantifying the amount of sulfur and potassium bound in the frozen slag layer. The findings of these laboratory studies are discussed and a general description of the slag deposit layers is given.

INTRODUCTION

The characterization of slag deposits which form within the Coal Fired Flow Facility (CFFF) test train has historically been a subject of interest since the beginning of active testing in this facility. This interest and need has been generated from the fact that slag deposits have a dominate effect on the performance of this test facility in terms of its heat transfer effectiveness, the durability of its flow components, and effective utilization of seed.

Past research at the University of Tennessee Space Institute (CFFF) and at other MHD test facilities has noted both advantages and disadvantages associated with the presence of a coal slag in the MHD power train (1-7). In the more general sense, those components of the MHD power plant which stand to be affected the most by slag coverage during operation are those of the MHD topping cycle. This region is subjected to heat transfer rates that can be extremely high and, in the case of the MHD generator, to electrical stresses that arise with powered operation. Aside from the known benefit of slag coverage to reduce heat transfer, the overall benefit of the presence of slag in the MHD generator during its operation is still an uncertainty. From a survey of literature and from practical experience, several advantages and disadvantages of slag can be cited. Some of the more obvious of these are recalled in the following paragraphs.

Coal slag is highly reactive and caustic. Internal surfaces of the MHD system which contact slag are subject to an accelerated chemical attack. These reactions are enhanced by the high temperature associated with the MHD plasma. As of yet, no common or inexpensive material (metal or refractory) has been found which can withstand chemical attack by liquid coal slag for long duration.

Slag is an electrochemical medium. It will sustain electrical-chemical processes leading to material disintegration. The electro-chemical processes can be significant in the MHD generator environment where the generator electric fields drive ion exchange. Electro-chemical attack is a known major factor which severely erodes metal electrodes.

Condensed slag is medium for seed capture/loss. Potassium becomes bound in the slag layer by both mechanical (mixing) means and through chemical reactions. Loss of seed to the slag reduces seeding effectiveness (seed utilization) which can subsequently reduce the MHD plasma conductivity. Also, chemical reactions between potassium and slag species can form insoluble potassium compounds which impact both the techniques and economy of seed regeneration schemes.

The slag layer increases near wall voltage drops. The presence of slag over the generator electrode surface can be viewed as a barrier to discharge of electrode current. In this context, the slag layer can increase electrode voltage losses/drops.

Metal ions and metal species which become bound in the slag can lend the slag layer electrically conducting. It has been demonstrated in experiments that over sustained time

*This work was supported by the U.S. Department of Energy, under Contract DE-AC02-79ET10815. Paper Number DOE/ET/10815-148.

periods of MHD generator operation that the slag layer can in fact become highly electrically conductive. The conductive slag layer can sustain axial (end-to-end) current leakage across the generator which compromises its electrical performance.

Slag can produce polarization. The natural migration of the plasma potassium ion in the presence of the generator electric field can drive ions into the cathode slag layer leading to charge polarization across the generator. Polarization is accompanied by an extremely conductive slag layer over the cathode surface. This conductive layer can electrically short out adjacent segmented cathode electrodes leading to a resegmentation of the cathode wall. Cathode shorting both degrades MHD generator performance and creates high voltage interelectrode gaps which are known to lead to enhanced destruction of electrode material.

The slag layer is a natural barrier to dynamic erosion of the wall surfaces. This layer constitutes a buffer layer which can reduce impact damage of high velocity particles.

Slag deposits reduce heat transfer. This final item can be interpreted as either an advantage or disadvantage of the slag layer since it is dependent upon whether benefits can be obtained by enhancing or reducing heat losses.

From the items discussed above, it is obvious that "the jury is still out" as to the exact benefit or deficit that slag imposes to the MHD power train. The component for which the most uncertainty exists is, of course, the generator.

However, the benefit of maintaining a stable slag layer within components that are subjected to high operational heat loads is one aspect of slag that is known. A steady state slag layer maintained over internal surfaces will substantially reduce the heat transfer. Slag acts as a thermal barrier between the plasma and the duct walls. This barrier both reduces component metal temperatures and plasma heat losses. The first of these effects can be conducive to increasing the serviceable lifetime of materials/hardware. The second reduces low grade heat losses of the power train, and, is in fact conducive to MHD electrical performance since plasma heat loss constitutes a major process inefficiency for the generator.

Consequently, slag coverage can enhance the durability and service life of test train components which are normally exposed to the high temperature, high velocity plasma. It is this particular advantage of the slag which is of practical interest to CFFF operations since this facility does not include an MHD generator in its test train. The Low Mass Flow (LMF) test train which is currently being testing at the CFFF incorporates an upstream flow train that is designed to thermodynamically simulate operation of the MHD topping cycle, that is, driven by operation with high pressure, high temperature coal-fired combustion essentially identical to that required to produce an MHD plasma.

Over the past year UTSI initiated and completed an extensive program to study slag deposition in the LMF test train. UTSI researchers have been collecting post test slag samples from the flow for intensive study. The objectives of this work has been to gain an increased understanding of factors which influence slag formation and to derive from this work any apparent correlation of the effect of slag deposits on the operation and lifetime of components. Particular emphasis of this work was placed on characterizing slag deposition in the upstream portion of the Low Mass Flow (LMF) test train. This information has been archived following the several long duration tests that were conducted at the CFFF during 1988 and 1989. This paper reports on major findings of these slag studies.

TEST FACILITY AND OPERATION

The CFFF is one of the two major U.S. MHD test facilities of the Department of Energy. Research in this facility is directed at conduct of proof-of-concept testing of the MHD power train bottoming cycle. The specific area of the national commercial power MHD research program that is being addressed at the CFFF is that of demonstrating the operation and performance of components of the MHD bottoming cycle. To achieve this mission, the general test scheme at this facility over the past two years has been to conduct long duration tests, that is, hundreds of hours of sustained operation at 20 Mwt.

The CFFF test train includes bottoming cycle components that allow for characterization of heat recovery and effluent control of the flue gas process stream. In addition to the bottoming cycle, the test train has in place an upstream test train which simulates thermodynamic operation typical to the MHD combustor and generator. This portion of the test train is that for which most of the slag sampling results of this paper are applicable.

The CFFF LMF upstream test train is shown schematically in Figure 1. This figure identifies each major component and can be used as a reference for other figures presented herein.

The major components of the upstream are the vitiation heater, coal-combustor, supersonic nozzle, supersonic aerodynamic duct, and the diffuser. In normal test operation, high pressure, high temperature substoichiometric combustion of pulverized coal, seeded with potassium, is used to produce a plasma typical for MHD. The high pressure plasma is subsequently accelerated through the nozzle to produce a supersonic flow stream which passes the length of the aerodynamic duct. The exhaust flow of the duct is conditioned within the diffuser and in turn exhausted into the radiant furnace of the downstream test train. Adjustment of the flow field to the back pressure requirement of the furnace is through the action of a flow field shockwave and flow diffusion.

The nominal 20 MWt test condition for the CFFF is summarized in Table 1 in terms of combustor operation (reactant flows and mixture ratios). The results of slag studies presented in this report were for tests using Illinois #6 coal with operation over sustained periods at this nominal condition. A gravimetric analysis of the composition of Illinois #6 coal, including its ash, is given in Table 2.

TABLE 1

CFFF NOMINAL 20Mwt COMBUSTOR OPERATING POINT

Reactants:	Coal - Illinois #6	0.365 kg/s
	Seed - K_2CO_3	0.047
	Oil - (#2 Fuel Oil)	0.193
	Air	1.528
	Oxygen	0.818
	Total Flow	2.951
Set Point:	Stoichiometry	0.85
	N/O (mass)	1.0
	Thermal Input	19 to 20 MWt
	Combustion Pressure	4.6 Atm
	Combustor-Nozzle Total Heat Loss	1.4MW

TABLE 2

ILLINOIS #6 COAL COMPOSITION

Element	%	Ash Analysis	% of Ash
Carbon	64.6	Al_2O_3	15.2
Hydrogen	4.6	CaO	4.5
Nitrogen	1.4	Fe_2O_3	20.1
Sulfur	3.5	K_2O	2.3
Moisture (Dried)	< 4.0	MgO	0.7
		Na_2O	1.0
Volatiles	43.6	SO_3	1.2
Ash	10.3	SiO_2	51.1
		TiO_2	0.9

Shown in Figure 2 are plots of the distribution of plasmadynamic variables along the upstream test train. These plots were computed for the flow within the aerodynamic duct and through the diffuser using a standard UTSI one dimensional plasmadynamic computer code (8). The theoretical results presented in this figure can be used to provide information on the general influence of plasmadynamic state on slag deposition.

Operating conditions applied for these calculations are consistent with the nominal operating point for the CFFF as presented in Table 1. Slag covered walls were assumed as a boundary condition in computing local heat transfer rates. The physical geometry of each section of the aerodynamic duct and each diffuser section was used. Discrete changes in wall divergence of the circular aerodynamic duct are present in the three sections which make up the duct length. These discrete geometric changes give rise to the discontinuities that are seen the calculations as the flow passes from one duct section to the other. Similarly, the diffuser is constructed with three sections, a constant area cylindrical duct/diffuser section which mates to the aerodynamic duct and two large, abrupt expansions sections.

The plasmadynamic variables presented in Figure 2 are those thermodynamic and fluid dynamic properties which are known to markedly influence slag deposition. The phenomena which have proven to be prominent factors affecting slag growth are the local heat transfer rate and the shear between the plasma and liquid slag layer interface. The general idea of the magnitude of both of these can be inferred from Figure 2, through a review of the plots of heat transfer and plasma temperature along with those of wall shear and plasma velocity. (Heat transfer data for the LMF4Q test which includes the combustor is presented in Figure 3.)

In general, these plasmadynamic distributions describe the nature of the supersonic-subsonic flow stream that exists in the CFFF test train through the upstream duct and the diffuser during normal 20 MWt operation. High velocity, high temperature and high heat transfer rate are evident essentially everywhere throughout the entire flow passage. In the supersonic portion of the aerodynamic duct, the flow is initially accelerated. This acceleration leads to an increase in the velocity and a decrease in both the static temperature and heat transfer rate along the aerodynamic duct. A distributed flow field shock system is predicted to situate in the aft end of the duct. This shock system forms in the third duct section and extends to the entrance of the first diffuser section. Downstream of the shock the flow nature changes abruptly as the flow regime is driven from supersonic to subsonic, that is, the temperature rises, the velocity decreases and the heat transfer is enhanced by increased radiation.

Slag Sampling and Analysis Techniques

As a general course of CFFF post test operating procedures, the slag layer within the upstream test train is always qualified by visual inspection and the results of this inspection are documented. In recent CFFF tests (LMF4Q and later), special shut down procedures were followed with the expressed objective of attempting to preserve the upstream slag layer. These procedures encompassed the abrupt shutdown of all reactant flows (normal shutdown procedures include step reduction in flows with a final period of operation with oil burning). The abrupt shutdown procedures left an intact, frozen slag layer on all the upstream component walls. This frozen slag layer is taken as being representative of the steady state layer which existed during hot-firing.

Upon disassembly of the upstream flow train following the LMF4Q test, samples of slag were extracted from fifty-two (52) locations. These locations ranged from inside the primary combustor and downstream through the secondary furnace. Where it was practical, four (4) samples were taken at each location - one on each wall/side of the components/ducts.

General analyses procedures followed for evaluating each slag sample included cataloging its extraction location and measurement and cataloging its thickness. In addition, a general qualifying of each sample for texture, color and other physical characteristics was made. More detailed analyses of the samples were made using the CFFF Scanning Electron Microscope (SEM). This instrument allowed for intrinsic viewing of the slag structure to distinguish the different layers which appeared to have been formed. A final analysis was conducted by CFFF Chemical laboratory. These SEM analyses were used to determine the quantitative chemical composition of the samples. Selected samples were examined for mineral content.

The chemical quantitative analyses was specifically directed at determination of the sulfur and potassium content of the slag samples. Slag samples from distributed locations along the test train were selected for chemical evaluation. In this fashion, a determination of the sulfur and potassium content with axial position in the test train was sought. As a parallel effort, various other aspects of the slag samples were correlated with operating conditions, i.e., heat transfer data and the theoretical thermodynamics of each major upstream component. Results of all of these types of studies are given in the following section.

TEST AND ANALYSES RESULTS

Slag Layer Thickness

The thickness of each slag sample was measured and recorded. Where multiple samples were taken at a single location, an average thickness was determined and this average is reported herein. Table 3 presents a tabulation of the thickness of the slag layer for each upstream component. The axial location relative to the combustor injector/disperser plate where these samples were extracted is also itemized.

In summary, it can be seen in these results that the nominal thickness of the slag deposits within the supersonic portion of the upstream (nozzle and aerodynamic duct) is on the order of 1.5 mm or less. Thicker deposits form in the low velocity regions (combustor and subsonic diffuser).

TABLE 3

SLAG SAMPLE THICKNESS FOR CFFF UPSTREAM COMPONENTS

Location/Upstream Component	Axial Distance (m)	Slag Layer Thickness (mm)
1 / Combustor Disperser Plate	0.00	1.02
2 / Combustor Cylindrical Chamber	0.08	3.73
3 / Combustor Conical Section	0.58	1.25
4 / Nozzle (Plate 1)	1.02	1.22
5 / Nozzle (Plate 3)	1.12	0.86
6 / Nozzle (Plate 4)	1.17	0.76
7 / Nozzle (Plate 5)	1.22	0.86
8 / Aerodynamic Duct (Section 1)	1.27	0.81
9 / Aerodynamic Duct (Section 1)	2.01	0.94
10 / Aerodynamic Duct (Section 2)	2.77	1.58
11 / Aerodynamic Duct (Section 3)	2.87	1.55
12 / Aerodynamic Duct (Section 3)	3.53	3.12
13 / Diffuser (Section 2)	5.08	3.20
14 / Diffuser (Section 3)	6.60	5.13
15 / Radiant Furnace	8.13	6.35
16 / Radiant Furnace	9.14	10.16

A plot of the tabulated results of Table 3 is presented in Figure 4. This plot provides a visual embellishment of the distribution of slag thickness with axial position along the LMF upstream. Probably the most noticeable feature of this plot is the characteristic slag layer growth which occurs from the nozzle downstream. This growth is reasonably well defined in these results and it has also been noted throughout testing with the current duct configuration. The general trend of slag growth through the aerodynamic duct and diffuser suggests that slag deposition is most likely dominated by the magnitude local heat transfer. This contention can be drawn from comparison of the distribution of slag thickness versus those for heat flux and velocity (Figure 2).

Figure 3 presents data from measurements of heat flux distribution over the upstream test train. By comparing the slag thickness plot of Figure 4 to the heat flux distribution of Figure 3 an inverse correlation between these two parameters can be inferred. This character can be anticipated since the amount of deposited slag that covers the duct walls markedly influences the heat transfer rate, and, vice versa. The slag thickness and heat transfer are cross plotted in Figure 5 to illustrate their relation. The slag layer tends to be thinner in the regions of high heat flux. This character is consistent with first order theoretical heat transfer considerations for steady state operation.

The steady state thickness that the slag deposits will achieve during nominal operation in the LMF test train is dependent upon a multitude of physical and operational variables. First of all, the physical and mechanical design of the duct must be considered. As was noted in the discussion of Figure 2, the flow duct of the upstream is assembled from duct sections which either discretely or abruptly vary in lofting. In addition to these lofting discontinuities, these sections also are fabricated with distinctly different materials (carbon steel and stainless steel cooling rings/internal surfaces) and each duct section is independently water cooled. Consequently, no well defined common ground exists for estimation of the heat transfer in relation to slag deposition.

Secondly, as was exhibited in Figure 2, the plasmadynamics within the upstream is by no means continuous. Abrupt changes in the flow field occur between duct sections and the presence of a flow shock system within the duct lends a mixed flow situation for the overall upstream. Taking into account the abrupt changes in plasma temperature, velocity and shear that occur between duct sections, similar discontinuities in the slag deposition can be anticipated.

As a consequence of these uncertainties, any attempt to obtain a reasonable prediction of the slag deposition and slag layer thickness in the LMF upstream is most likely futile. Rather empirical data such as those provided in this research is of greater value in interpretation of the effects of slag on performance, heat transfer and durability.

Slag Chemical Composition

Table 4 presents a general tabulation of the chemical composition of CFFF slag samples. This tabulation gives upper and lower limits on the amounts of the various slag oxides species that were present in all samples - the average amount is also given. In this table, no distinction has been made as to the axial position where slag samples were taken - the values quoted are rather global results of all upstream samples.

The slag composition for two CFFF LMF tests (LMF4P and LMF4Q) is compared in Table 4. These compositions are in turn compared to slag data of Farrar et. al., which was published at the 27th Symposium on Engineering Aspects of Magnetohydrodynamics (3). The referenced data were reported for Illinois #6, coal-fired tests at the Component Development and Integration Facility (CDIF). These data are from chemical evaluations of slag taken from the cathode wall of the CDIF MHD generator.

It is interesting to note that all composition data of Table 4 compare favorably. A consistency in the mineral content between the CDIF slag samples and those of the CFFF tests is apparent. A special note is made of the fact that the level of potassium bound in the slag for both data sets is quite similar. Whereas the CDIF cathode slag data set is subject to an electric field, the CFFF data set is not. The relevance of this result is not certain. However, it does suggest that a more detailed, statistical comparison between the potassium content of slag deposits in the MHD generator versus that for unpowered channel may be enlightening.

TABLE 4

CHEMICAL ANALYSIS OF CFFF LMF SLAG SAMPLES

Species		LMF4P %	LMF4Q %	CDIF Data* %
SiO_2	min	33.05	34.70	
	max	41.85	45.23	
	ave	38.60	39.40	38.10
Al_2O_3	min	13.18	17.13	
	max	18.72	21.61	
	ave	15.58	18.90	18.50
Fe_2O_3	min	10.11	9.12	
	max	15.75	16.60	
	ave	13.07	14.01	15.60
TiO_2	min	0.40	0.61	
	max	0.73	1.28	
	ave	0.54	0.83	0.90
CaO	min	3.60	1.88	
	max	7.25	3.78	
	ave	5.60	2.86	2.40
MgO	min	0.61	0.53	
	max	1.49	0.83	
	ave	0.98	0.69	0.90
Na_2O	min	0.45	0.20	
	max	0.54	0.52	
	ave	0.50	0.32	1.00
K_2O	min	17.61	15.45	
	max	29.28	28.68	
	ave	21.44	20.88	22.70
SO_3	min	0.29	0.05	
	max	3.69	2.56	
	ave	1.62	0.69	0.50

* Data of Reference 3 - Illinois #6 Coal

Figure 6 shows the concentrations of the major chemical species of the slag samples plotted against axial location along the LMF upstream flow train from which they were extracted. Only slight variation in the amounts/ concentration for most all chemical species is apparent. This finding applies to both the slag bound sulfur and potassium. In fact, only small, trace amounts of sulfur were found to be present in all the slag samples that were chemically analyzed.

SEM Analyses

Slag samples from each major upstream component were viewed with the SEM. These analyses provided an evaluation of the structure and general texture of the slag at various locations in the test train. SEM photographs of varying magnification level for slag samples taken in the combustor, the duct, and the diffuser are reviewed.

From "eyeball" observations of the slag and from the SEM studies, three distinctive layers could be distinguished in each slag sample. These layers tend to conform to the accepted model of slag deposition and are sketched and identified in Figure 7. It was noted in detailed study of the slag that the presence, degree and nature of these layers varied with location along the test train.

As illustrated in Figure 7, the three layers are coined as the deposit layer (next to the wall), the solid/frozen slag layer, and the liquid layer which interfaces the plasma stream. Each of these layers is discussed in turn in the following paragraphs with emphasis on the findings of this study with regard to each.

Deposit Layer. In the analyses of the CFFF samples, it was seen that the deposit layer was extremely thin (< 0.2 mm) and brittle. It tended to be powdery and flake off when handled. Care must be exercised in sample extraction to assure retention of this layer. It was also noted in chemical analyses that this layer contained sulfur. In some cases most all the sulfur content of the entire slag sample was confined within this layer. From this observation and from the general difference in the physical character of this layer from the others, it is contended that the probability of this layer forming over the walls prior to combustion of coal is high. Normal test procedures followed in operation of the CFFF include a initial warmup period of the entire system wherein the combustor is fired with oil. This warmup period can extend for up to one hour or more. The deposit layer is not unlike that seen as wall residue typical to combustion of oil.

Solid/Frozen Slag Layer. Visual and SEM evaluations of this layer in the CFFF slag samples showed it to be of an amorphous texture (containing voids and channels). It is contended that this layer represents that portion of the slag deposit which must have existed as a solid during steady state operation. The solidification point for Illinois #6 slag is approximately 1530K (2,7). Consequently, the defined interface between this layer and the liquid layer approximates the isotherm for slag solidification. (Nominal operating temperatures of between 500K to 800K for metal surfaces within the upstream duct have been monitored in past tests.)

Liquid Slag Layer. Analysis of this layer showed it to be considerably denser than the other slag layers. This uppermost (i.e., furthest away from the wall) layer is hypothesized to be that portion of the slag deposit that existed as liquid during steady state operation. As such this layer is dynamic and flows down the channel being driven by the action of fluid dynamic shear. (Intact recovery of this type of layer can only be achieved by an abrupt shutdown, such as was instituted for this purpose in the LMF4Q test.) This layer is also that interface into which slag condensation/mass transfer from the plasma takes place.

The thickness that each of the above described layers achieve is dependent upon thermodynamic and dynamic conditions within the test train component. Whereas, slag can be expected to condense and solidify to some degree over highly cooled walls, the amount of liquid slag deposit that can be sustained at various locations along the duct length is dependent upon the local dynamic conditions. The ability of the liquid slag to flow is a major factor effecting slag deposition. This ability is determined by its viscosity which is exponentially dependent upon temperature(6,7). As much as a two fold increase in viscosity can be anticipated between the condensation and solidification temperature bounds of liquid slag.

In the same context, the condensation of slag on cold walls required to initiate and sustain deposition is dependent on the flow dynamics. The steady state thickness represents a net deposition rate determined by the rate at which mass is transferred from the plasma and the rate at which it is swept away with the flow. Consequently, the thickness of the liquid layer and the general steady state thickness for the entire composite slag layer is dependent upon two principal aspects of the flow, the rate of heat transfer and the velocity. Bearing these aspects in mind, qualification of the slag deposits on the various components of the CFFF upstream can be reasonably interpreted.

Figure 8 is an SEM photograph showing a 30x magnification of a typical slag sample extracted for the side of the CFFF primary combustion chamber. In this photograph, the three characteristic layers described above are quite obvious. The liquid layer of this sample is appreciable thick and was observed to be very dense. This layer exhibited a vitreous-crystalline structure quite similar to glass. The solid layer was noted to be extremely porous.

Composition analysis of the combustor sample was made at six point locations across it thickness. These points are annotated with letters A through F in Figure 8. Sulfur content in this sample was only noted at point F (within the deposit layer). Essentially no sulfur was apparent in any of the other zones. Overall, the density of the combustor sample was approximately 3.2 to 3.7 g/cc.

Figure 9 presents an SEM photograph of 54x magnification of a slag sample taken in the LMF nozzle. A deposit layer for this sample was not discernible. The composition analysis of this sample did not indicate the presence of any sulfur. A precise definition of the interface between the liquid and solid slag was not possible in this sample.

Consequently, in overall texture this sample must be classified as intermediate to that nominal for the liquid and solid layers. The sample was essentially nonporous. A quantification of the density of this sample was in the 2.4 to 2.6 g/cc range. This is considerably less than that determined for the combustor sample.

The final SEM photograph presented in Figure 10 shows a 32x magnification of a slag sample that was collected from the last diffuser section graph, near the furnace entrance. It can be seen by comparison of this photo to those of the previous figures, that this sample is obviously different. Although a definition of the interface between the liquid and solid layers can be readily distinguished, even the liquid layer is amorphous in structure. This character is considerably different than that which was observed for the combustor slag sample. Chemical analysis of this sample showed the presence of sulfur only at the wall interface point (E). This sample also exhibited the highest percentage of bound potassium over the other samples analyzed. Samples taken in the diffuser and furnace regions had densities around 2.5 to 2.7 g/cc.

CONCLUDING REMARKS

The research work that has been reported herein was undertaken at the initiative of UTSI staff with the expressed objective of increasing the understanding of slag deposition in the CFFF LMF test train. And, in this regard the findings of these studies are considered to be unique to this system and should not be construed as applicable in the general sense.

The slag analyses techniques employed in this work varied from documentation of gross observations of the slag made by the individuals of this research team to precise CFFF laboratory quantitative chemical analyses. Subject to this type of hands-on research, in conjunction with historical supporting research at the CFFF that has been conducted on slag characterization, it is believed that a reasonable understanding of slag formation and its effects on the performance of the LMF test train has been acquired.

Some of the major points reported herein concerning this research are reemphasized in the following brief statements:

1) The chemical composition of the slag layer in the upstream CFFF flow train was very constant along its entire length.

2) Potassium bound in the slag was greater in the diffuser.

3) Overall sulfur concentration in the form of SO_3 was very low and the major concentration of the sulfur was within the thin deposit layer adjacent to the duct walls.

4) The chemical composition of the Illinois #6 slag in the CFFF was found to be nearly identical to that reported last year for samples taken from the cathode wall of the CDIF generator.

5) Correlation between slag thickness measurements for samples at distributed locations along the upstream test train and theoretical local plasmadynamic state was noted. These data suggest that the heat flux is the strongest major factor influencing slag deposition throughout most all of the CFFF upstream test train.

6) A descriptive model of slag deposits consisting of three layers: a deposit layer next to the duct wall, a solid layer and a liquid layer was used and formed the basis for evaluation of SEM studies. The nature of these layers and the general structure and texture of the slag was noted to vary from component to component of the CFFF upstream.

REFERENCES

1) Crawford, L. W., et al., "Investigation of Slag Deposits and Seed Absorption in a Direct-Fired MHD Power Generator", 6th Int'l. Conf. on Magnetohydrodynamic Power Generation, Washington, DC, 1975.

2) Koester, J. K., et al., "In-Channel Observations of Coal Slag", 15th SEAM, Univ. of PA, Philadelphia, PA, 1976.

3) Farrar, L. C., Pollina, R. J., and Rosa, R. J., "Effects of Coal Slag on MHD Channel Electrical Behavior", 27th SEAM, Reno, NV, 1989

4) Webster Capps, "Some Properties of Coal Slags of Importance to MHD", 16th SEAM, Pittsburgh, PA, 1977.

5) Rodgers, M. E., Arressohn, P. C. and Kruger C. H., "Comparison of Measurements and Prediction of the Fluid Mechanics and Thermal Behavior of MHD Channel Slag Layers", 16th SEAM, Pittsburgh, PA, 1977.

6) Pian, C. C. P and Smith, J. M., "Velocity and Temperature Distributions of Coal Slag Layers on Magnetohydrodynamic Generator Walls", Lewis Research Center, Cleveland, OH, 1977.

7) Rodgers, M. E. and Kruger, C. H., "Fluid Mechanics and Thermal Behavior of MHD Channel Slag Layers", 17th SEAM, Stanford University, Palo Alto, CA, 1978.

8) Lineberry, J. T. and Galanga F. L., "Gas Dynamic and Heat Transfer Evaluations of the CFFF LMF1 Flow Train," 21st SEAM, Argonne Nat'l. Lab., Argonne, IL, July 1983.

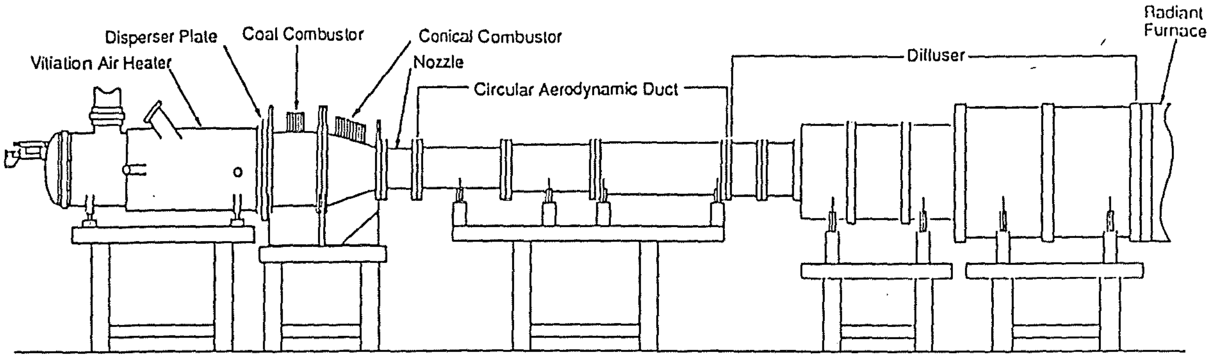

Figure 1. CFFF LMF Upstream Flow Train

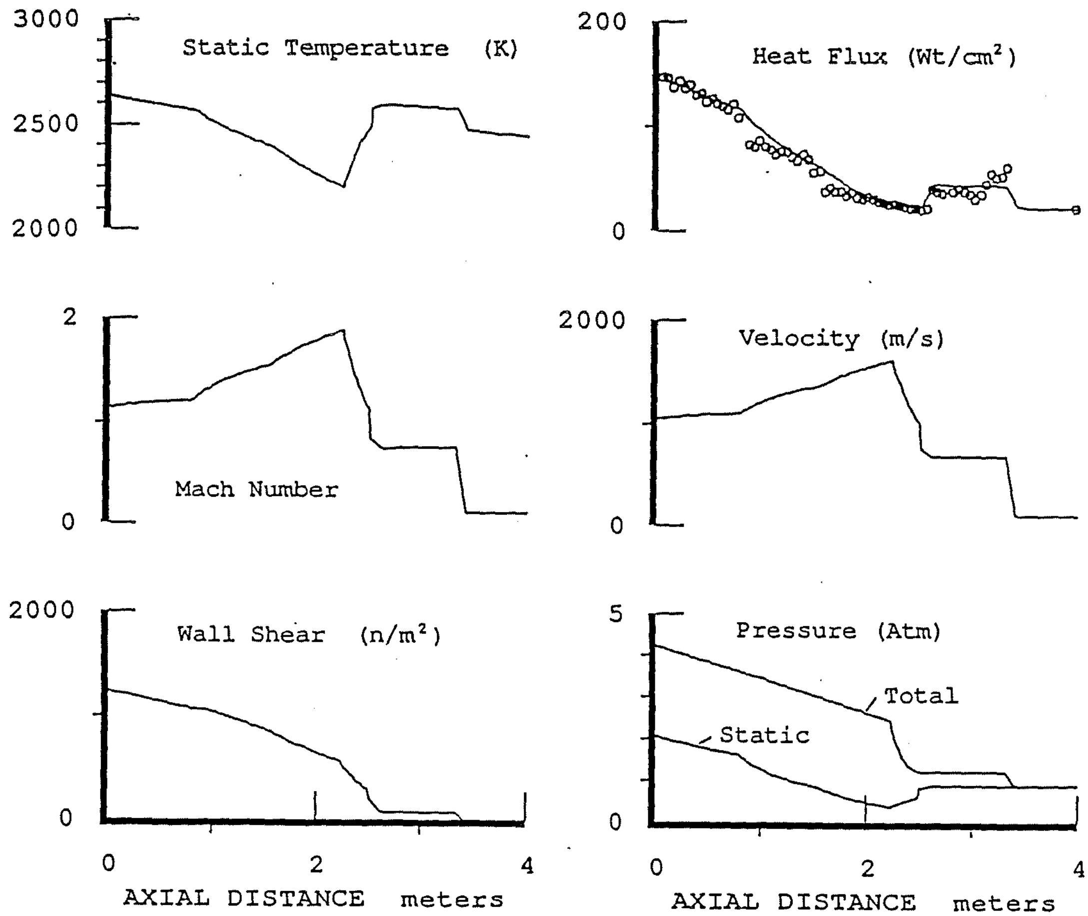

Figure 2. CFFF LMF Upstream Plasmadynamics

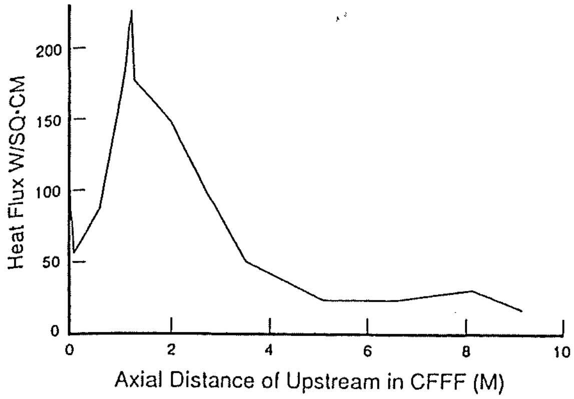

Figure 3. Measured Heat Flux Distribution in CFFF Upstream Test Train

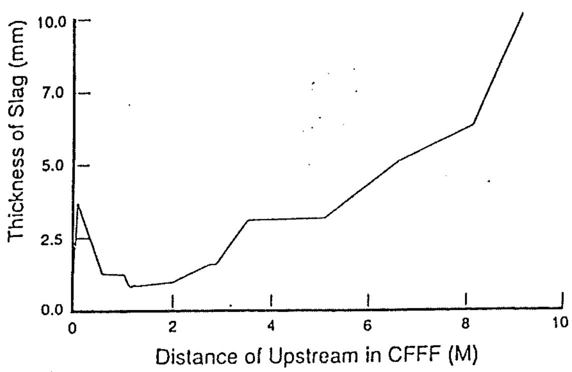

Figure 4. Measured Distribution of Slag Layer Thickness in Upstream CFFF LMF Test Train

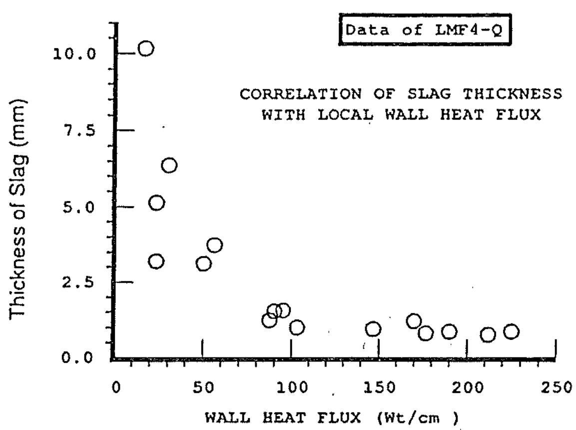

Figure 5. Crossplot of Measured Slag Layer Thickness with Measured Heat Flux - CFFF LMF Upstream Test Train

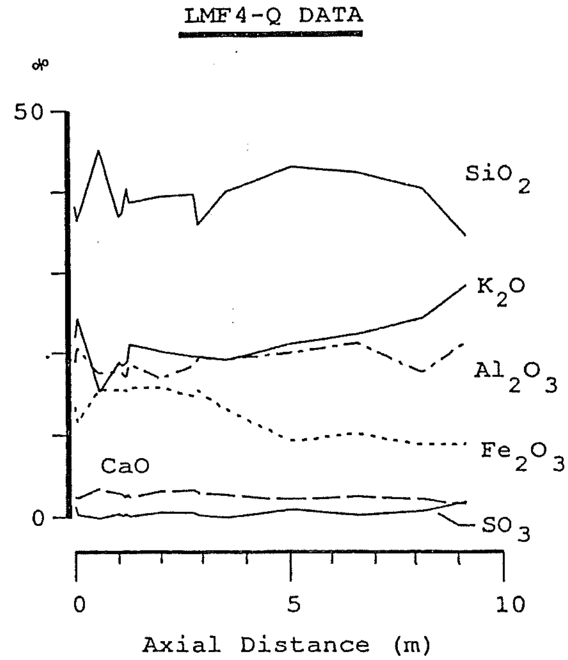

Figure 6. Axial Distribution of Slag Species Concentrations Along CFFF LMF Upstream Test Train

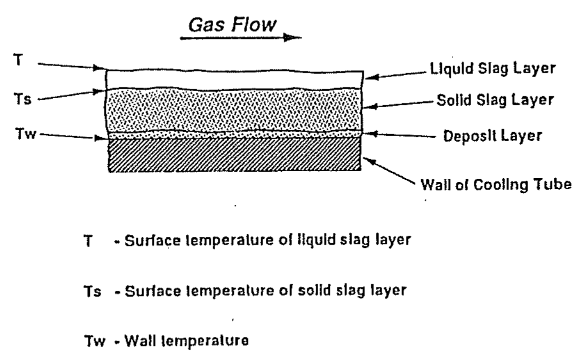

Figure 7. Sketch of General Slag Layer Structure

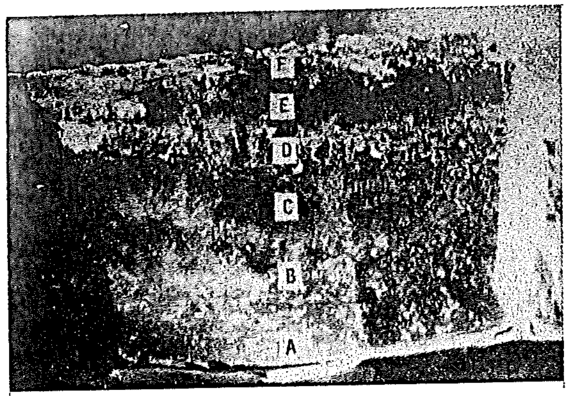

Figure 8. SEM Photograph of Combustor Slag Sample

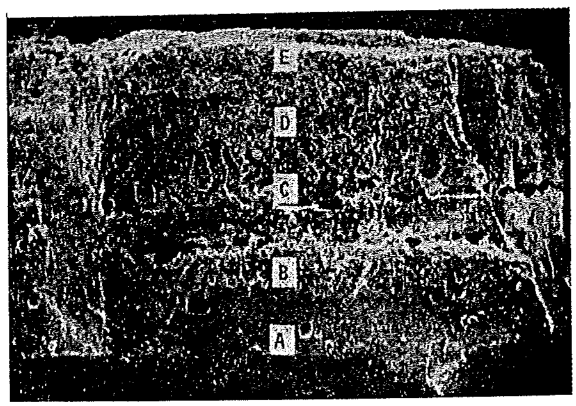

Figure 9. SEM Photograph of Nozzle Slag Sample

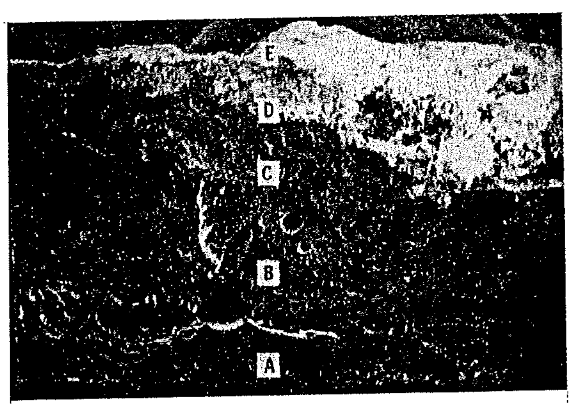

Figure 10. SEM Photograph of Diffuser Slag Sample